JCTC Journal of Chemical Theory and Computation

Geometry Optimization with Multilayer Methods Using Least-Squares Minimization

Wenkel Liang,[†] Craig T. Chapman,[†] Michael J. Frisch,[‡] and Xiaosong Li*,[†]

Department of Chemistry, University of Washington, Seattle, Washington 98195-1700, United States and Gaussian Incorporated, 340 Quinnipiac Street, Building 40, Wallingford, Connecticut 06492, United States

Received August 13, 2010

Abstract: In this article, we introduce a least-squares minimization scheme for optimizing molecular structures with mixed quantum mechanics (QM) and molecular mechanics (MM) multilayer models. A mixed-coordinate optimization framework was developed. The QM and MM regions are modeled with redundant internal coordinates and Cartesian coordinates, respectively. Within this mixed-coordinate system, a least-squares minimization method using the quasi-Newton step as the evaluation of error is constructed. The couplings between layers are treated rigidly in accordance with the mechanical embedding approach, and the MM Hessian is approximated as a scalar constant of the root-mean-square QM Hessian eigenvalues. Both two-layer and three-layer models were tested. The performance of the method developed herein shows consistently stable and fast convergence.

I. Introduction

Computational science has been very successful in many research areas, including chemistry, physics, materials, and biology. Computational efforts are applied to large systems of ever increasing size, such as biomolecules, polymers, and nanostructures with hundreds to thousands of atoms and electrons. Molecular mechanics, which scales linearly with respect to the system size at the cost of computational accuracy, is often the method of choice for large-scale systems. On the other hand, as the accuracy becomes more and more important in computational research, there is a strong need for using first-principles based methods for studying electronic structures of large systems. However, the requirement of computational resources for this need has outpaced advances in computer hardware because ab initio calculations scale nonlinearly with respect to the system size. A method that strikes a better balance between computational cost and accuracy is the mixed quantum mechanics and molecular mechanics (QM/MM) model[1−4] or the ONIOM model, which has shown enormous success in biochemical research fields (see refs 5−9 for recent reviews on QM/MM). In the QM/MM model, first-principles methods are used to describe electronic structures of chemically important subspaces while the rest of system is modeled by molecular mechanics force field theories. The interaction between these two subspaces is treated with embedding methods, such as the mechanical and electrostatic embedding approaches.

While energetics calculations based on the QM/MM or ONIOM model have been well defined in the literature, geometry optimization methods for such models are less frequently addressed, due to a 2-fold difficulty. First, the MM subspace often consists of thousands of atoms. An optimization method must be able to handle such a large geometric space efficiently and at an affordable computational cost. Second, optimization of the QM subspace is often carried out in internal coordinates with redundancy,[10−13] while the MM subspace is described by nonredundant Cartesian coordinates. Geometry optimization in such a mixed-coordinate space is generally difficult, and an algorithm often treats the two subspaces independently.[14−18] For example, the microiteration algorithm assumes that the QM subspace is stationary when optimizing the MM region. A conventional quasi-Newton based optimization method is then taken to optimize the QM region while holding the MM region intact.[19] Such an optimization scheme is rather successful and has become the standard for optimization of multilayer

* Corresponding author e-mail: li@chem.washington.edu.
[†] University of Washington.
[‡] Gaussian Incorporated.

10.1021/ct100453x
Published on Web 10/12/2010

mixed QM and MM models. A more recent effort by Vreven et al. computes explicit coupling between QM and MM layers in the Hessian matrix.[20] This approach is very useful in transition-state searches but is generally computationally expensive due to the explicit computation and handling of the full second-derivative matrix.

In this article, we introduce a different optimization concept for QM/MM or ONIOM models. We will present a geometry optimization algorithm that optimizes both QM and MM subspaces simultaneously. The underlying motivation is to develop a method that is generalized to be able to handle a mixed-coordinate system and is essentially independent of the construction or division of the system into layers. The following notations will be used in this article extensively: $\mathbf{R}$ and $\mathbf{g_R}$ are vector and energy gradients in the general coordinate subspace; $\mathbf{Q}$ and $\mathbf{g_Q}$ are vector and energy gradients in redundant internal coordinates for the quantum mechanical (QM) subspace; $\mathbf{X}$ and $\mathbf{g_X}$ are vector and energy gradients in Cartesian coordinates for the molecular mechanical (MM) subspace; $\{c_i\}$ are variational parameters for the least-squared minimization; $\mathbf{H}$ is the Hessian (energy second derivatives).

II. Algorithm

In the search space defined by $\{\mathbf{R}_i\}$, an optimization algorithm can be designed to look for a new vector $\mathbf{R}^*$ that is associated with the minimal error. One of the most popular forms of the desired new vector in geometry and wave function optimization is the linear combination of the search space

$$\mathbf{R}^* = \sum_i c_i \mathbf{R}_i \text{ and } \sum_i c_i = 1 \tag{1}$$

With the definition of the new vector in eq 1, an associated error function $f(\mathbf{R}^*)$ can be constructed. Minimizing the square of $f(\mathbf{R}^*)$ with respect to variational coefficients $\{c_i\}$ leads to a set of coupled equations, which can be solved for $\{c_i\}$ that minimize f.[2] Optimization algorithms using eq 1 as the new vector are often referred to as the direct inversion in the iterative subspace (DIIS) method.[21−24]

The key to the success of the DIIS algorithm is the choice of error function. In the context of geometry optimization, the error function f can be a measure of energy ΔE,[25−27] gradient $\mathbf{g}$,[21,22] or distance $\Delta\mathbf{R}$[23,24,27] to the minimum on the local potential energy surface (PES). In the current paper, the following error function is considered

$$f(\mathbf{R}^*) = \sum_{i=1}^{k} c_i \Delta\mathbf{R}_i \tag{2}$$

Equation 2 uses the distance $\Delta\mathbf{R}$ to the local minimum as an evaluation of the error. $\Delta\mathbf{R}$ can be calculated with the Newton−Raphson or quasi-Newton approach

$$\Delta\mathbf{R}_i^T = -\mathbf{g}_i^T \cdot \mathbf{H}^{-1} \tag{3}$$

The stability of the quasi-Newton approach can be enhanced by controlling the step size using the rational function optimization technique (RFO)[28,29] or the trust radius model (TRM).[30−36] According to the nature of this method, we will refer to it as quasi-Newton-DIIS (QN-DIIS). Minimization of eq 2 can be performed in a least-squares sense, written in a linear algebraic equation in matrix form[22]

$$\begin{pmatrix} a_{1,1} & \dots & a_{1,k} & 1 \\ \vdots & \ddots & \vdots & \vdots \\ a_{k,1} & \dots & a_{k,k} & 1 \\ 1 & \dots & 1 & 0 \end{pmatrix} \begin{pmatrix} c_1 \\ \vdots \\ c_k \\ \lambda \end{pmatrix} = \begin{pmatrix} 0 \\ \vdots \\ 0 \\ 1 \end{pmatrix} \tag{4}$$

where $a_{i,j} = (\mathbf{g}_i^T \cdot \mathbf{H}^{-1}) \cdot (\mathbf{g}^T{}_j \cdot \mathbf{H}^{-1})^T$. Solving eq 4 is computationally trivial, and the solution $\{c_i\}$ minimizes the square of the error function in eq 2. Equations 1−4 illustrate the least-squares minimization approach for geometry optimization with a uniform coordinate system. For a mixed-coordinate system, such as those described by the QM/MM or ONIOM model, the QM and MM subspaces are represented by the internal ($\mathbf{Q}$) and Cartesian ($\mathbf{X}$) coordinates, respectively. Internal coordinate space is known for its fast convergence, as it is a natural choice for molecular structures and vibrations. However, internal coordinate spaces are often associated with a large number of redundancies. Such redundancy is certainly not computationally cost effective for the large MM subspace, which often includes thousands of atoms. Therefore, a widely used approach is to represent the MM subspace using the Cartesian coordinates. We herein define a generalized QM/MM or ONIOM coordinate space

$$\mathbf{R} = (\mathbf{Q}\ \mathbf{X})^T \tag{5}$$

$$\mathbf{g} = (\mathbf{g_Q}\ \mathbf{g_X})^T \tag{6}$$

The DIIS search space is then defined by $\{\mathbf{R}_i\}$ as usual.

The QN-DIIS approach as described in eqs 1−4 requires computation of the Hessian

$$\mathbf{H} = \begin{pmatrix} \mathbf{H_{QQ}} & \mathbf{H_{QX}} \\ \mathbf{H_{XQ}} & \mathbf{H_{XX}} \end{pmatrix} \tag{7}$$

where $\mathbf{H_{QQ}}$ and $\mathbf{H_{XX}}$ are Hessian matrices for the QM and MM subspaces, respectively, and $\mathbf{H_{QX}} = \mathbf{H_{XQ}}$ are related to the couplings between these two subspaces. For the relatively small QM subspace, computationally expensive analytical evaluations of the second derivatives are replaced with a numerical Hessian update scheme, such as BFGS,[37−40] SR1,[41] and PSB,[42,43] to obtain an accurate QM Hessian $\mathbf{H_{QQ}}$. However, due to its large dimension, calculation and manipulation of the MM Hessian $\mathbf{H_{XX}}$ are not computationally practical. One simple approach is to approximate $\mathbf{H_{XX}}$ as a scaled identity matrix $\alpha \cdot \mathbf{I}$. In this implementation, the MM weighting factor α takes on the following form

$$\alpha = \sqrt{\frac{\sum_i^M \lambda_{ii}^2}{M}} \tag{8}$$

where λ's are the Hessian eigenvalues of the QM subspace and M is the number of nonredundant QM coordinates. Equation 8 is constructed in order to equally weigh both QM and MM subspaces in the DIIS equation.

In principle, the off-diagonal coupling term $\mathbf{H_{QX}}$ in eq 7 needs to be computed explicitly as it gives rise to the interaction between the two subspaces. Within the framework of QM/MM or ONIOM, various embedding approaches are used to treat the two subspaces independently via linking atoms and/or electrostatic point charges. To some extent, such a treatment implicitly decouples the QM and MM subspaces. Therefore, one can conveniently choose $\mathbf{H_{QX}} = 0$ in eq 7.

With approximations described above, eq 7 can be rewritten as

$$\mathbf{H} = \begin{pmatrix} \mathbf{H_{QQ}} & 0 \\ 0 & \alpha \cdot \mathbf{I} \end{pmatrix} \tag{9}$$

The quasi-Newton step in the QM/MM space can be defined as

$$\Delta \mathbf{R}^T = -\mathbf{g}_\mathbf{Q}^T \cdot \mathbf{H}_\mathbf{QQ}^{-1} - \mathbf{g}_\mathrm{X}^\mathrm{T} \cdot \alpha^{-1} \tag{10}$$

With this definition, the QN-DIIS equation (eq 4) can be easily constructed and solved and an optimization step can be taken as

$$\mathbf{R}_{N+1} = \mathbf{R}^* + \Delta \mathbf{R}^* = \sum_{i=1}^{N} c_i \cdot \mathbf{R}_i - \sum_{i=1}^{N} c_i \cdot \mathbf{g}_i^T \cdot \mathbf{H}^{-1} \tag{11}$$

The performance of the optimization scheme using DIIS critically depends on the quality of the approximated Hessian. Negative or saddle point Hessians are generally difficult to correct using the DIIS method. In the GDIIS method previously developed by Farkas,[24] additional controls on the direction and step size of the DIIS step were implemented. These controls were used to correct for possible bad Hessian approximations and to ensure a downhill optimization. In this implementation, these controls were replaced by using the standard RFO approach to preoptimize the structure into a near quadratic potential well with a positive definite Hessian in the spirit of the hybrid optimization method.[26] Nevertheless, the QN-DIIS method implemented here is formulary equivalent to the GDIIS method in ref 24. On the other hand, one could, in principle, use the energy-based linear squares minimization approach, such as the GEDIIS method.[26] However, the GEDIIS approach for mixed-coordinate systems is not ideal in this scenario mainly because changes of energy in the Cartesian coordinate system along various degrees of freedom are strongly coupled.

After the RFO approach preoptimizes the structure to near-quadratic well, the overall optimization algorithm for QM/MM proceeds as follows. Gradients for both QM and MM subspaces are computed in the Cartesian coordinates. The QM Cartesian gradients are transformed into the internal coordinate space. The QM Hessian is updated, and the MM scaling factor α is calculated (eqs 8 and 9). The quasi-Newton step of the whole QM/MM or ONIOM space is constructed for all saved points using the current Hessian (eq 10). The DIIS equation is solved, and a new optimization step is taken (eq 11). The QM internal coordinates are transformed back to the Cartesian coordinates for gradient calculations. MM microiterations are carried out so that MM gradients are at the same convergence level as the QM gradients ($\mathbf{g_X} \leq \mathbf{g_Q}$).

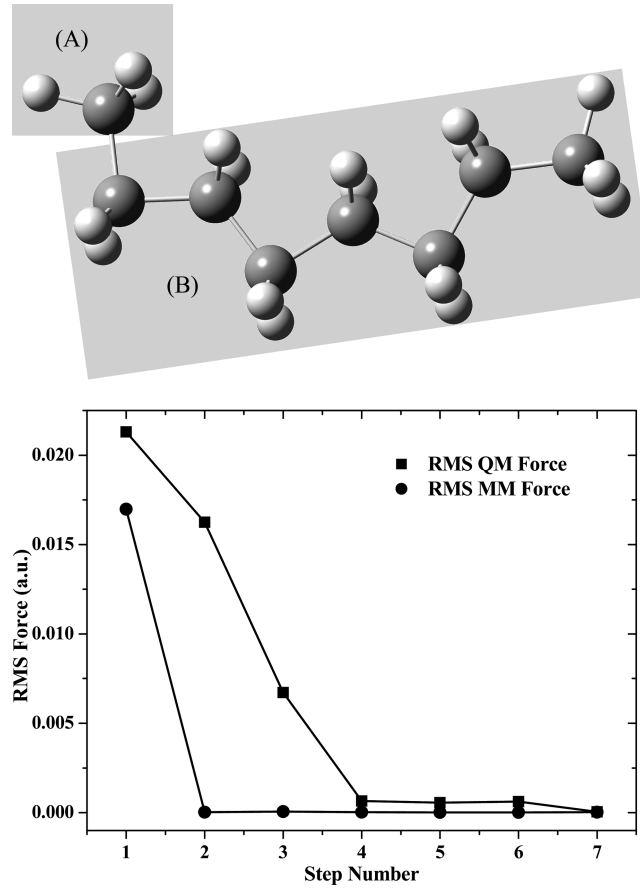

Figure 1. Force convergence profiles during optimizations of the two-layer ONIOM model of C_8H_{18}. Layer A is modeled with the HF/STO-3G level of theory, and layer B is modeled with the Amber[45] force field.

III. Benchmarks and Discussion

Optimizations were carried out on a SGI Atlix 450 workstation (Intel dual core-Itanium 1.6 GHz with 48GB of RAM) using the development version of the GAUSSIAN[44] suite of programs with the implementation of the QM/MM optimization algorithm presented here. For all methods tested here, the optimization is considered converged when the maximum **g** is less than 0.00045 au, the root-mean-square (rms) **g** is less than 0.00030 au, the maximum $\Delta\mathbf{R}$ is less than 0.0018 au, and the rms $\Delta\mathbf{R}$ is less than 0.0020 au. The hybrid optimization scheme is used in this work. Simple RFO steps are taken to search for a good local potential well before the DIIS algorithm is used to optimize the system to the minimum (see refs 26 and 27 for details). Usually, the initial RFO search for a local potential well takes one-third to one-fifth of the total number of geometry optimization steps.

The first test case is a two-layer model of the C_8H_{18} molecule (Figure 1) using the ONIOM approach. The embedding method is mechanical with hydrogen as the linking atom. In this model, the ending methyl group is modeled with the HF/STO-3G level of theory, while the rest of system is modeled with Amber force field theory. Convergence profiles of rms $\mathbf{g_Q}$ and $\mathbf{g_X}$ are plotted in Figure

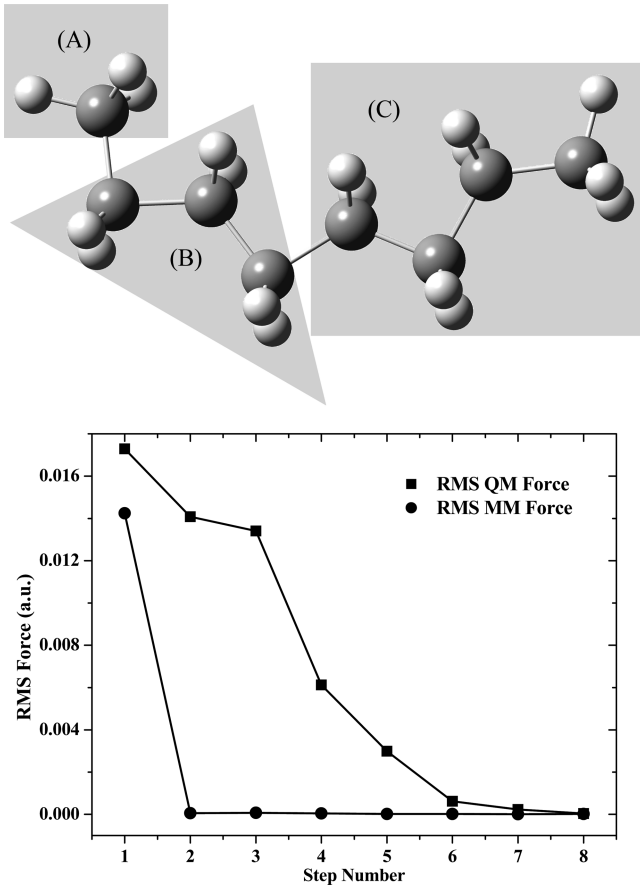

Figure 2. Force convergence profiles during optimizations of the three-layer ONIOM model of C_8H_{18}. Layer A is modeled with the B3LYP/STO-3G level of theory; layer B is modeled with the HF/STO-3G level of theory; layer C is modeled with the Amber[45] force field.

1. As described in the previous section, several MM microiterations using the conjugated gradient method are carried out in each optimization step. As a result, the rms $\mathbf{g}_X$ converges faster than the rms $\mathbf{g}_Q$. The overall optimization profile is smooth and efficient for this two-layer test case. Optimizations for three-layer ONIOM systems are more difficult as the middle layer is often connected to both the higher and lower layers. Such a situation adds an implicit constraint and complexity to the optimization problem. Figure 2 depicts a three-layer ONIOM model for the C_8H_{18} molecule, where B3LYP/STO-3G, HF/STO-3G, and Amber force field theories are used to model the three layers. As an extension to the method described above, all QM layers are treated as independent subspaces, provided with the analytical first derivatives and updated Hessians for each layer. The couplings between QM layers are through the mechanical embedding method with hydrogen as the linking atom. The full gradient and Hessian for such a three-layer case can be written as

$$\mathbf{g} = (\mathbf{g}_{Q\text{-I}}\ \mathbf{g}_{Q\text{-II}}\ \mathbf{g}_X)^T \tag{12}$$

$$\mathbf{H} = \begin{pmatrix} \mathbf{H}_{QQ-I} & 0 & 0 \\ 0 & \mathbf{H}_{QQ-II} & 0 \\ 0 & 0 & \alpha\cdot\mathbf{I} \end{pmatrix} \tag{13}$$

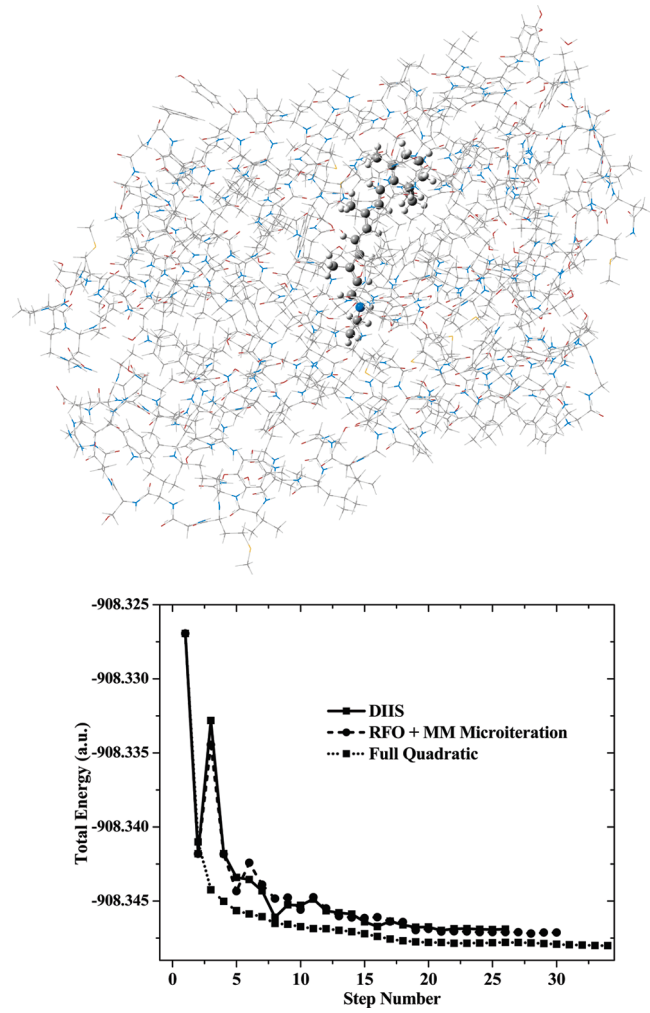

Figure 3. Comparison of optimization energy profiles using the multiplayer DIIS, conventional RFO, and full quadratic approaches for the two-layer ONIOM model of bacteriorhodopsin. The high-level layer (ball-and-stick) is modeled with the B3LYP/3-21G level of theory; the low-level layer (wire-frame) is modeled with the Amber[45] force field.

where $\mathbf{H}_{QQ\text{-I}}$ and $\mathbf{H}_{QQ\text{-II}}$ are updated Hessians for the two QM layers and α is computed using eq 8 with a summation over all QM variables. The performance of the optimization method introduced here for a three-layer ONIOM model is shown in Figure 2. With the three-layer ONIOM model, the optimization method also exhibits smooth and fast convergence behavior similar to that of a two-layer model. For both two-layer and three-layer models, the fast convergence of the MM force at the beginning of the optimization process is a result of the microiteration approach for the MM region. The importance of the DIIS approach comes into play at the later stage of the optimization when both QM and MM layers are in the near-quadratic potential well. For the test cases presented herein (Figures 1 and 2), the DIIS optimization scheme starts from the fourth step.

Figure 3 shows a two-layer ONIOM model for the bacteriorhodopsin. In this system, there are 3568 atoms modeled by Amber force field and 56 atoms by B3LYP/3-21G. The test is compared with the conventional RFO approach with microiterations to fully converge the MM layer at each step and the full quadratic method.[20] All three

methods considered here are able to converge such a large system within a reasonable number of steps (<34 geometry steps). Since the energy difference between the three optimized structures is <0.5 kcal/mol, they are considered to be at the same potential minimum. The optimization pathways are very similar in both RFO and DIIS test cases as they are quasi-Newton approach based methods. There are a number of unproductive oscillations at the beginning of the optimization process exhibited by both the RFO and the DIIS approaches. This is due to a lack of explicit coupling in the full Hessian between layers. On the other hand, with a proper treatment of the coupling, the full quadratic optimization is very smooth, however, at a much higher computational cost. The overall computational cost taken by the full quadratic optimization is more than three times that of the RFO or DIIS approach. While both RFO and DIIS methods take a similar number of steps to finish the test job and converge to a same minimum, the multilayer DIIS methods costs less than the conventional RFO method. In the multiplayer DIIS method, the MM region does not need to be converged at each optimization step because the MM geometry errors are taken into account in the least-squares minimization scheme. As a result, the overall computational savings using the method introduced here is about 25% compared to that of using the RFO method with microiterations.

IV. Conclusion

In this article, we introduced a method for optimizing molecular structures with multilayer models, such as QM/MM and ONIOM. A mixed-coordinate least-squares optimization framework was developed and generalized for QM and MM regions represented by redundant internal coordinates and Cartesian coordinates, respectively. Both two-layer (QM:MM) and three-layer (QM:QM:MM) models were tested. The performance of the method developed herein shows consistently smooth and fast convergence.

Acknowledgment. This work was supported by the U.S. National Science Foundation (CHE-CAREER 0844999 to X.L.). Additional support from Gaussian Inc. and the University of Washington Student Technology Fund is gratefully acknowledged.

References

(1) Warshel, A.; Levitt, M. *J. Mol. Biol.* **1976**, *103*, 227.

(2) Singh, U. C.; Kollman, P. A. *J. Comput. Chem.* **1986**, *7*, 718.

(3) Field, M. J.; Bash, P. A.; Karplus, M. *J. Comput. Chem.* **1990**, *11*, 700.

(4) Gao, J. *Acc. Chem. Res.* **1996**, *29*, 298.

(5) Gao, J.; Truhlar, D. G. *Annu. Rev. Phys. Chem.* **2002**, *53*, 467.

(6) Shurki, A.; Warshel, A.; Valerie, D. Structure/Function Correlations of Proteins using MM, QM/MM, and Related Approaches: Methods, Concepts, Pitfalls, and Current Progress. In *Advances in Protein Chemistry*; Academic Press: New York, 2003; Vol. 66, pp 249.

(7) Friesner, R. A.; Guallar, V. *Annu. Rev. Phys. Chem.* **2005**, *56*, 389.

(8) Vreven, T.; Morokuma, K.; David, C. S. Hybrid Methods: ONIOM(QM:MM) and QM/MM. In *Annual Reports in Computational Chemistry*; Elsevier: New York, 2006; Vol. 2, p 35.

(9) Senn, H. M.; Thiel, W. *Angew. Chem., Int. Ed.* **2009**, *48*, 1198.

(10) Fogarasi, G.; Zhou, X. F.; Taylor, P. W.; Pulay, P. *J. Am. Chem. Soc.* **1992**, *114*, 8191.

(11) Pulay, P.; Fogarasi, G. *J. Chem. Phys.* **1992**, *96*, 2856.

(12) Peng, C. Y.; Ayala, P. Y.; Schlegel, H. B.; Frisch, M. J. *J. Comput. Chem.* **1996**, *17*, 49.

(13) Liang, W.; Wang, H.; Hung, J.; Li, X.; Frisch, M. J. *J. Chem. Theory Comput.* **2010**, *6*, 2034.

(14) Maseras, F.; Morokuma, K. *J. Comput. Chem.* **1995**, *16*, 1170.

(15) Humbel, S.; Sieber, S.; Morokuma, K. *J. Chem. Phys.* **1996**, *105*, 1959.

(16) Svensson, M.; Humbel, S.; Morokuma, K. *J. Chem. Phys.* **1996**, *105*, 3654.

(17) Dapprich, S.; Kom·romi, I. n.; Byun, K. S.; Morokuma, K.; Frisch, M. J. *J. Mol. Struct. THEOCHEM* **1999**, *461*−*462*, 1.

(18) Vreven, T.; Byun, K. S.; Komáromi, I.; Dapprich, S.; Montgomery, J. A.; Morokuma, K.; Frisch, M. J. *J. Chem. Theory Comput.* **2006**, *2*, 815.

(19) Vreven, T.; Morokuma, K.; Farkas, d.; Schlegel, H. B.; Frisch, M. J. *J. Comput. Chem.* **2003**, *24*, 760.

(20) Vreven, T.; Frisch, M. J.; Kudin, K. N.; Schlegel, H. B.; Morokuma, K. *Mol. Phys.* **2006**, *104*, 701.

(21) Pulay, P. *Chem. Phys. Lett.* **1980**, *73*, 393.

(22) Pulay, P. *J. Comput. Chem.* **1982**, *3*, 556.

(23) Csaszar, P.; Pulay, P. *J. Mol. Struct.* **1984**, *114*, 31.

(24) Farkas, Ö.; Schlegel, H. B. *Phys. Chem. Chem. Phys.* **2002**, *4*, 11.

(25) Kudin, K. N.; Scuseria, G. E.; Cancès, E. *J. Chem. Phys.* **2002**, *116*, 8255.

(26) Li, X.; Frisch, M. J. *J. Chem. Theory Comput.* **2006**, *2*, 835.

(27) Moss, C. L.; Li, X. *J. Chem. Phys.* **2008**, 129.

(28) Banerjee, A.; Adams, N.; Simons, J.; Shepard, R. *J. Phys. Chem.* **1985**, *89*, 52.

(29) Simons, J.; Nichols, J. *Int. J. Quantum Chem.* **1990**, *24*, 263.

(30) Fletcher, R. *Practical Methods of Optimization*; Wiley: Chichester, 1981; p 95.

(31) Gill, P. E.; Murray, W.; Wright, M. H. *Practical Optimization*; Academic: New York, 1981; p 114.

(32) Powell, M. J. D. *Non-linear Optimization*; Academic: New York, 1982; p 29.

(33) Dennis, J. E.; Schnabel, R. B. *Numerical Methods for Unconstrained Optimization and Nonlinear Equations*; Prentice Hall: New York, 1983; p 129.

(34) Scales, L. E. *Introduction to Non-linear Optimization*; Springer-Verlag: New York, 1985; p 115.

(35) Schlegel, H. B.; Yarkony, D. R. Geometry optimization on potential energy surfaces. *Modern Electronic Structure Theory*; World Scientific: Singapore, 1995; p 459.

(36) Schlegel, H. B.; Schleyer, P. v. R.; Allinger, N. L.; Kollman, P. A.; Clark, T.; Schaefer, H. F., III; Gasteiger, J.; Schreiner, P. R. Geometry optimization. In *Encyclopedia of Computational Chemistry*; Wiley: Chichester, 1998; Vol. 2, pp 1136.

(37) Broyden, C. G. *J. Inst. Math. Appl.* **1970**, *6*, 76.

(38) Fletcher, R. *Comput. J. (Switzerland)* **1970**, *13*, 317.

(39) Goldfarb, D. *Math. Comput.* **1970**, *24*, 23.

(40) Shanno, D. F. *Math. Comput.* **1970**, *24*, 647.

(41) Murtagh, B.; Sargent, R. W. H. *Comput. J. (Switzerland)* **1972**, *13*, 185.

(42) Powell, M. J. D. *Nonlinear Programing*; Academic: New York, 1970; pp 31.

(43) Powell, M. J. D. *Math. Program.* **1971**, *1*, 26.

(44) Frisch, M. J.; Trucks, G. W.; Schlegel, H. B.; Scuseria, G. E.; Robb, M. A.; Cheeseman, J. R.; Scalmani, G.; Barone, V.; Mennucci, B.; Petersson, G. A.; Nakatsuji, H.; Caricato, M.; Li, X.; Hratchian, H. P.; Izmaylov, A. F.; Bloino, J.; Zheng, G.; Sonnenberg, J. L.; Hada, M.; Ehara, M.; Toyota, K.; Fukuda, R.; Hasegawa, J.; Ishida, M.; Nakajima, T.; Honda, Y.; Kitao, O.; Nakai, H.; Vreven, T.; Montgomery, J. A.; Peralta, J. E.; Ogliaro, F.; Bearpark, M.; Heyd, J. J.; Brothers, E.; Kudin, K. N.; Staroverov, V. N.; Kobayashi, R.; Normand, J.; Raghavachari, K.; Rendell, A.; Burant, J. C.; Iyengar, S. S.; Tomasi, J.; Cossi, M.; Rega, N.; Millam, J. M.; Klene, M.; Knox, J. E.; Cross, J. B.; Bakken, V.; Adamo, C.; Jaramillo, J.; Gomperts, R.; Stratmann, R. E.; Yazyev, O.; Austin, A. J.; Cammi, R.; Pomelli, C.; Ochterski, J. W.; Martin, R. L.; Morokuma, K.; Zakrzewski, V. G.; Voth, G. A.; Salvador, P.; Dannenberg, J. J.; Dapprich, S.; Parandekar, P. V.; Mayhall, N. J.; Daniels, A. D.; Farkas, O.; Foresman, J. B.; Ortiz, J. V.; Cioslowski, J.; Fox, D. J. *Gaussian Development Version H.09+*; Gaussian, Inc.: Wallingford, CT, 2010.

(45) Cornell, W. D.; Cieplak, P.; Bayly, C. I.; Gould, I. R.; Merz, K. M.; Ferguson, D. M.; Spellmeyer, D. C.; Fox, T.; Caldwell, J. W.; Kollman, P. A. *J. Am. Chem. Soc.* **1995**, *117*, 5179.

CT100453X